Signature of criticality in angular momentum resolved entanglement of scalar fields in $d > 1$

Mrinal Kanti Sarkar,* Saranyo Moitra,† and Rajdeep Sensarma
Department of Theoretical Physics, Tata Institute of Fundamental Research, Mumbai 400005, India

(Received 17 September 2023; revised 21 May 2024; accepted 25 June 2024; published 13 August 2024)

The scaling of entanglement entropy with subsystem size fails to distinguish between the gapped and the gapless ground states of a scalar field theory in $d > 1$ dimensions. We show that the scaling of the angular momentum resolved entanglement entropy S_ℓ with the subsystem radius R can clearly distinguish between these states. For a massless theory with momentum cutoff Λ, $S_\ell \sim \ln[\Lambda R/\ell]$ for $\Lambda R \gg \ell$, while $S_\ell \sim R^0$ for the massive theory. In contrast, for a free Fermi gas with Fermi wave vector k_F, $S_\ell \sim \ln[k_F R]$ for $k_F R \gg \ell$. We show how this leads to an "area-log" scaling of total entanglement entropy of fermions, while the extra factor of ℓ leads to a leading area law even for massless bosons. At finite temperatures, we find that there is a crossover in the scaling of S_ℓ from the $T = 0$ logarithmic scaling to a high T linear scaling $S_\ell \sim \pi T R/3$. The logarithmic scaling exists for larger subsystem sizes for larger values of ℓ. We provide estimates of temperatures and subsystem sizes where this critical scaling can be seen in experiments on ultracold atoms.

DOI: 10.1103/PhysRevB.110.075128

I. INTRODUCTION

The scaling of entanglement entropy with the size of the subsystem [1–13] can provide strong indications about the nature of the underlying quantum state in a many-body system. For a generic thermal state, the entanglement entropy scales with the "volume" of the subsystem [1,14,15] (i.e., $S \sim R^d$ for a subsystem of linear size R in d spatial dimensions). Entanglement entropy of gapped ground states [12,16–18] as well as excited states in many-body localized systems [19–23] scale with the "area" of the subsystem (i.e., $S \sim R^{d-1}$). Quantum scars [24,25] have a logarithmic scaling with subsystem size. Subleading scaling of entanglement entropy can also be used to identify gapped topological phases [6–8]. Dynamics of entanglement entropy can also reveal the nature of the underlying quantum system [19,26–28].

Entanglement scaling in gapless ground states is more complicated. In $d = 1$, gapless ground states (e.g., free massless scalar [29–32] fields as well as the free Fermi gas [33,34]) show a logarithmic scaling of entanglement entropy with the subsystem size ($S \sim \ln R$), with a universal prefactor [10–12,32,35,36] determined by the central charge of the 1+1D[1] conformal field theory. For $d > 1$, the answers vary: Entanglement entropy of free fermions shows an "area-log" scaling [33,34,37–40], $S \sim R^{d-1} \ln R$. However, the ground state of massless scalar fields shows an area law entanglement scaling [17,41–43] in spite of being a gapless conformally invariant system. The leading-order scaling of entanglement entropy does not show any signature of the gapless state, although subleading corrections can indicate the presence of criticality [35,42]. This raises the following question: Why does the leading entanglement scaling of critical bosons not leave any signature in $d > 1$?

In $d > 1$, ground states of both massless and massive scalar fields show area law [4,12,16–18,44] scaling of entanglement, with a nonuniversal prefactor which depends on the mass and the high-energy regularization of the theory. One can ask: Is there any entanglement entropy related quantity whose leading-order scaling with the subsystem size clearly distinguishes between the gapped and the gapless states of the scalar field theory in $d > 1$?

In this paper, we answer both the questions raised above by considering the entanglement of a rotationally invariant "spherical" subsystem A of radius R centered at the origin in the ground state of a free scalar field theory in 2+1D and 3+1D with a momentum cutoff Λ. The entanglement entropy S is a sum of entropies in each angular momentum channel ℓ, i.e., $S = \sum_\ell g_\ell S_\ell$, where $g_\ell = 1\,(2)$ for $\ell = 0\,(\ell > 0)$ in 2+1D and $g_\ell = (2\ell + 1)$ in 3+1D. S_ℓ is thus the symmetry resolved entanglement [45,46] for rotational invariance.

We first focus on the ground state ($T = 0$):

(a) For massless scalar fields in both 2+1D and 3+1D, $S_\ell \sim \frac{1}{6} \ln[\Lambda R/2\ell]$ for $\ell \ll \Lambda R$. The logarithmic scaling of S_ℓ with $\Lambda R/\ell$ with a universal prefactor hints at an effective 1+1D CFT for each angular momentum channel. For massive theories, $S_\ell \sim R^0$ in this limit. Thus, the scaling of S_ℓ with subsystem size can clearly distinguish between gapless and gapped ground states for scalar fields in $d > 1$. We note that starting from the pioneering work of Srednicki [41], previous works [16,17,42,47] on entanglement entropy in scalar fields have always used angular momentum decomposition. However, the scaling of S_ℓ was not considered in these works. Only recently, Huerta *et al.* [48] have used CFT arguments to derive the scaling for S_ℓ.

(b) For a massless scalar field, $S(\Lambda R)$ gets substantial contributions from S_ℓ only for $\ell < \ell_c$, where $2\ell_c = \Lambda R$. The $\ln \Lambda R$ contribution from each ℓ channel leads to a leading area-log scaling, but this is exactly canceled by the

*Contact author: mrinal.sarkar@tifr.res.in
†Contact author: smoitra@theory.tifr.res.in

[1]We will use d for spatial dimensions and D for space-time dimensions.

contribution of the $\ln \ell$ term. This leaves behind a contribution that scales with the "area" of the subsystem. Our scaling form for the angular momentum resolved entanglement entropy reproduces the subleading constant term in 2+1D CFT and the subleading logarithmic term in 3+1D CFT for total entanglement entropy.

(c) For comparison, we also calculate S_ℓ for a free Fermi gas with Fermi wave vector k_F in $d = 2$ and $d = 3$. Here S_ℓ is suppressed for $\ell \gg k_F R$ and $S_\ell \sim \frac{1}{6} \ln [k_F R]$ for $k_F R \gg \ell$. In this case, there is no cancellation: The number of channels scale as $(k_F R)^{d-1}$ and hence $S \sim (k_F R)^{d-1} \ln [k_F R]$. For scalar fields, the extra scaling by ℓ in the logarithm for S_ℓ hides the signature of the gapless phase in the scaling of S, which becomes apparent when we look at scaling of individual S_ℓ s. Our results should also apply to leading order in an interacting $O(N)$ theory in the large N limit [43], where they can be used to track the quantum phase transition in the system [43,49].

While entanglement entropy has firmly established itself in the lexicon of quantum many-body systems, it is notoriously hard to measure in experiments. In an early experiment [50], entanglement of a bosonic system was measured where the Hilbert space was partitioned between states with even and odd occupation numbers. However, entanglement with a spatial partition, which is key to our undrstanding of entanglement scalings, have been hard to measure. This is partly due to the fact that experiments are usually geared towards measuring correlation functions and the dictionary between correlations and entanglement is not fully understood. Recently, the entanglement entropy of $1d$ bosons have been measured in ultracold atomic systems [51] by measuring the correlation functions of both the bosonic fields and their conjugate momenta, using interference of identical systems. The spatially resolved information about the correlation functions is then used in formulas for entanglement entropy of free bosons to measure the entanglement entropy of these systems. Since one starts from the full knowledge of spatial variations of the measured correlation functions, in $2d$ or $3d$, one can easily construct the angular momentum resolved correlators by using appropriate spherical harmonics. This can then be put in formulas for angular momentum resolved entanglement entropy (given in this paper) to measure S_ℓ in these systems.

However, the experiments operate at a finite temperature, and hence it is important to consider whether any remnant of the $T = 0$ logarithmic scaling of S_ℓ can be seen at finite temperatures. In general, for subsystem sizes R much smaller than the thermal wavelength $\lambda_{\rm th} = \hbar c/T$, where c is the speed of the waves corresponding to the scalar field, dephasing of quantum correlations due to thermal fluctuations can be ignored and one would expect to see the $T = 0$ logarithmic scaling. For $R \gg \lambda_{\rm th}$, one expects a linear scaling with subsystem size in high-temperature limit. We calculate S_ℓ for the critical scalar field at $T \neq 0$ and find that (a) for $\Lambda R < 2\ell$, $S_\ell \sim 0$; (b) for $2\ell < \Lambda R < \Lambda R_c(\ell)$, $S_\ell \sim (1/6) \ln [\Lambda R/\ell]$; and (c) for $R \gg R_c(\ell)$, $S_\ell \sim \frac{\pi T R}{3}$, which is the high-temperature scaling answer for a 1+1D CFT [29]. Interestingly, we find that crossover scale $R_c(\ell)$ increases with ℓ. Thus, it would be easier to see the logarithmic scaling of S_ℓ in experimental settings for intermediate ℓ values (for very large values of ℓ, the short distance cutoff beyond which logarithmic scaling is seen would grow).

We finally consider ultracold atomic gases of bosons [52–54] and estimate the temperature ranges and subsystem sizes where the critical logarithmic scaling may be seen. We find that the estimates are just at the boundaries of feasibility with current ultracold atomic gases experiments.

This paper is organized as follows: In Sec. II, we consider the angular momentum resolution of correlation functions and relate S_ℓ to these correlators. Then, in Sec. III, we looked at scaling behavior of S_ℓ in ground states of massive and massless scalar field theories. Here we show how S_ℓ can clearly distinguish between these theories. In Sec. IV, we understand why the critical scaling of S_ℓ fails to leave a signature in the scaling of total entanglement entropy. For this, we compare the situation with free fermions, where logarithmic scaling of S_ℓ does lead to an "area-log" scaling of entanglement. In Sec. V, we study the finite-temperature crossover of S_ℓ from logarithmic to linear scaling behavior and estimate experimental parameters for ultracold atomic gases where this critical scaling may be seen. Finally, we end with a summary of our results in Sec. VI.

II. ANGULAR MOMENTUM RESOLVED ENTANGLEMENT ENTROPY OF SCALAR FIELDS

The action for a free scalar field theory in d dimensions is

$$\begin{aligned}\mathcal{S} &= \int d^d\mathbf{r} \int dt \phi(\mathbf{r},t)\left[-\partial_t^2 + \nabla^2 - m^2\right]\phi(\mathbf{r},t) \\ &= \int_0^\Lambda \frac{d^d\mathbf{k}}{(2\pi)^d} \int \frac{d\omega}{2\pi} \phi(\mathbf{k},\omega)[\omega^2 - |\mathbf{k}|^2 - m^2]\phi(-\mathbf{k},-\omega),\end{aligned} \tag{1}$$

where m is the mass, and we have defined the theory with an ultraviolet momentum cutoff Λ to get finite answers for entanglement entropy. Λ^{-1} can be considered as a minimum grid size or short distance cutoff in real space for this system. The spectrum of the theory is given by $\omega_{\mathbf{k}} = \sqrt{|\mathbf{k}|^2 + m^2}$, and $m = 0$ corresponds to the gapless or the critical theory.

The von-Neumann entanglement entropy of free scalar fields can be calculated in terms of its correlation functions within the subsystem [2,17,55], i.e.,

$$S = \mathrm{Tr}_A\left[\frac{(\hat{M}+1)}{2}\ln\frac{(\hat{M}+1)}{2} - \frac{(\hat{M}-1)}{2}\ln\frac{(\hat{M}-1)}{2}\right], \tag{2}$$

where the trace is over coordinates in subsystem A. Here

$$\hat{M}^2(\mathbf{r},\mathbf{r}') = \int_{\mathbf{r}_1\in A} d^d\mathbf{r}_1\, M^+(\mathbf{r},\mathbf{r}_1)\, M^-(\mathbf{r}_1,\mathbf{r}'),$$

with the equal time correlators of the fields and their conjugate momenta,

$$\begin{aligned} M^+(\mathbf{r},\mathbf{r}') &= \langle \phi(\mathbf{r},t)\,\phi(\mathbf{r}',t)\rangle \\ &= \int_0^\Lambda \frac{d^d\mathbf{k}}{(2\pi)^d} \frac{e^{i\mathbf{k}\cdot(\mathbf{r}-\mathbf{r}')}}{\omega_{\mathbf{k}}} \coth\left[\frac{\omega_{\mathbf{k}}}{2T}\right], \\ M^-(\mathbf{r},\mathbf{r}') &= \langle \dot{\phi}(\mathbf{r},t)\,\dot{\phi}(\mathbf{r}',t)\rangle \\ &= \int_0^\Lambda \frac{d^d\mathbf{k}}{(2\pi)^d}\, \omega_{\mathbf{k}}\, e^{i\mathbf{k}\cdot(\mathbf{r}-\mathbf{r}')} \coth\left[\frac{\omega_{\mathbf{k}}}{2T}\right]. \end{aligned} \tag{3}$$

Here T is the temperature of the system.

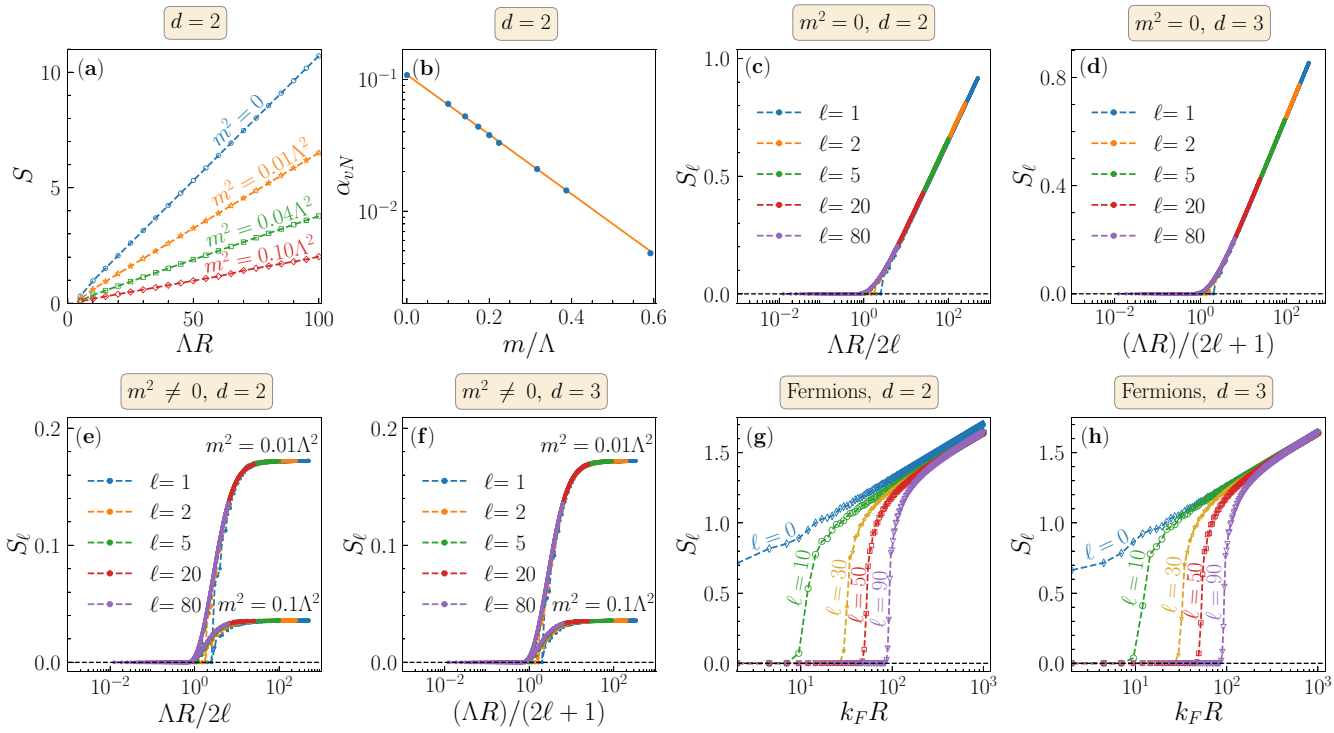

FIG. 1. Scaling of entanglement entropy with subsystem size for scalar field theory [(a)–(f)] and free Fermi gas [(g) and (h)]. (a) Area law scaling of $S = \alpha_{vN}(\Lambda R) + \text{const.}$ for a scalar field theory in 2+1D for massless as well as massive systems. (b) α_{vN} as a function of m/Λ showing exponential decrease of α_{vN} with m. Note that α_{vN} is nonuniversal and depends on regularization scheme. (c) Logarithmic scaling of $S_\ell \sim \frac{1}{6}\ln[\Lambda R/2\ell]$ for a 2+1D massless scalar field and (d) $S_\ell \sim \frac{1}{6}\ln[\Lambda R/(2\ell+1)]$ for a 3+1D massless scalar field. Note the data collapse for different ℓ channels. This scaling feature of S_ℓ is independent of regularization schemes. (e) Scaling of S_ℓ with $\Lambda R/2\ell$ for different ℓ channels for a massive 2+1D scalar field theory with $m^2 = 0.01\Lambda^2$ and $m^2 = 0.1\Lambda^2$. S_ℓ goes to a constant at large ΛR. The constant value decreases with increasing m. (f) Scaling of S_ℓ with $\Lambda R/(2\ell+1)$ for massive scalar fields in 3+1D. The behavior is similar to that in (e). [(g) and (h)] Logarithmic scaling of S_ℓ with $k_F R$ for a Free fermi gas in $d = 2$ (g) and $d = 3$ (h). Note the absence of the extra scale factor of ℓ in this case.

We consider a "spherical" subsystem of radius R centered at the origin. For this rotationally invariant subsystem, the correlators $M^{\pm}$ and hence $\hat{M}^2$ are block diagonal in the angular momentum channels ℓ. This reduces the complexity to solving many one-dimensional problems in the radial coordinates. In this case, it is easy to see that $S = \sum_\ell g_\ell S_\ell$, where $g_\ell = 1\,(2)$ for $\ell = 0\,(\ell > 0)$ for $d = 2$ and $g_\ell = 2\ell + 1$ in $d = 3$.[2] The ℓ^{th} channel entanglement entropy is

$$S_\ell = \text{Tr}_r\left[\frac{(\hat{M}_\ell+1)}{2}\ln\frac{(\hat{M}_\ell+1)}{2} - \frac{(\hat{M}_\ell-1)}{2}\ln\frac{(\hat{M}_\ell-1)}{2}\right], \tag{4}$$

where Tr_r indicates trace only over radial coordinates in A. Here $\hat{M}^2_\ell(r,r') = \int_0^R dr_1\, r_1^{d-1}\; M^+_\ell(r,r_1)\; M^-_\ell(r_1,r')$, where

$$M^{\pm}_\ell(r,r_1) = \frac{1}{(rr_1)^\nu}\int_0^\Lambda \frac{k\,dk}{\omega_k^{\pm 1}}\, J_{\ell+\nu}(kr)\, J_{\ell+\nu}(kr_1)\coth\left[\frac{\omega_k}{2T}\right], \tag{5}$$

with $\nu = (d-2)/2$ and $J_n(x)$ is the Bessel function of the first kind of order n. The continuum operator $\hat{M}^2_\ell$ has eigenvalues $\lambda_n \geqslant 1$ [2,17,56]. To compute S_ℓ, we evaluate $\hat{M}^2_\ell(r,r')$ on a discrete set of radial points to construct a finite-dimensional matrix, but only consider $\lambda_n \geqslant 1$ to compute the required trace in Eq. (4). We note that in his early paper on entanglement entropy of scalar fields, Srednicki [41] had considered angular momentum decomposition of the field equations and regularized the resulting radial equations on a lattice. However, the scaling of S_ℓ was not considered in that paper. We have also considered this alternate lattice regularization scheme, where the radial fields are discretized on a lattice of finite length [16,41,42]. We find that the universal answers which we focus on here (e.g., logarithmic scaling of S_ℓ with universal coefficients) remain unchanged whether one uses a lattice regularization or simply uses the $\lambda_n > 1$ eigenvalues. This is discussed in detail in Appendix A. Nonuniversal features like coefficient of area law scaling of total entanglement entropy, which are known to depend on details of regulariza-

[2]We note that this requires the bosonic dispersion to be isotropic as well. If the bosonic dispersion is anisotropic, say $w_k = \sqrt{k_x^2 + \alpha^2 k_y^2}$, then one can work with the scaled variable $\tilde{k}_y = \alpha k_y$ to make it isotropic. To keep the phases in the Fourier transforms invariant, one would have to use $\tilde{y} = y/\alpha$ as scaled variable in the real space. If the subsystem is an ellipse with ellipticity $1/\alpha$, i.e., $x^2 + \frac{y^2}{\alpha^2} = R^2$, one can then again use angular momentum decomposition in scaled coordinates.

tion, are different in the two schemes (see Appendix A for details).

III. SCALING OF S_ℓ AT $T = 0$

Let us first focus on entanglement entropy of the subsystem at $T = 0$, where $\coth\left[\frac{\omega_k}{2T}\right] = 1$. In Fig. 1(a), we plot the total entanglement entropy S as a function of ΛR for 2+1D scalar fields. We find the well-known area law scaling $S = \alpha_{vN}(\Lambda R)$ + const. for both massless and massive fields, with a nonuniversal α_{vN} which rapidly decreases with increasing m [see Fig. 1(b)]. One can use a different regularization scheme, where the radial fields are defined on a discrete lattice [41]. While the area law is robust, the value of α_{vN} will differ in the two schemes.

We now consider S_ℓ for different values of ℓ as a function of the dimensionless size of the subsystem ΛR for a 2+1D scalar field theory. In Fig. 1(c), we plot S_ℓ for a massless scalar field theory as a function of $\Lambda R/2\ell$ for different values of ℓ. For $\Lambda R/2\ell \gg 1$, the curves for different ℓ (other than $\ell = 0$) collapse on top of each other. The curve is linear when plotted on a logarithmic scale for $\Lambda R/2\ell$, with a slope which is numerically found to be 1/6. Thus we find

$$S_\ell \sim \frac{1}{6} \ln\left[\frac{\Lambda R}{2\ell}\right] \tag{6}$$

for $\ell \neq 0$ and $S_\ell \sim \frac{1}{6} \ln[\Lambda R]$ for $\ell = 0$. We have checked that this scaling is independent of regularization schemes (see Appendix A). The logarithmic scaling of S_ℓ has recently been obtained by Huerta *et al.* [48] using CFT arguments. The universal prefactor of 1/6 hints at an underlying 1+1D CFT for the radial modes, with spatial coordinates scaled by the angular momentum quantum number ℓ. However, while the equation of motion for the radial modes has a global scale invariance, they do not have conformal invariance in these coordinates due to the presence of the centrifugal barrier. Note that this is the leading scaling of S_ℓ in a spherical subsystem, and it is distinct from the subleading logarithmic scaling of S in a subsystem with sharp corners [57–60]. We can contrast this with the scaling of S_ℓ for massive scalar fields. In Fig. 1(e), we plot S_ℓ as function of $\Lambda R/2\ell$ (on logarithmic scale) for $m^2/\Lambda^2 = 0.01$ and $m^2/\Lambda^2 = 0.1$. In both cases, we find that the S_ℓ curves for different ℓ values collapse on top of each other for $\Lambda R/2\ell \gg 1$. The curves rise linearly for intermediate ranges of ΛR, mimicking the logarithmic behavior of the critical theory, but settle down to a constant value for the largest subsystem sizes. Thus, $S_\ell \sim R^0$ for a massive theory. The constant value, which decreases with increasing m, is nonuniversal and depends on the regularization scheme. This is consistent with the fact that the system appears critical until the subsystem size is larger than the correlation length $\xi \sim 1/m$ in the system.

We note that the scaling of S_ℓ is not specific to 2+1D. A similar logarithmic scaling with the same prefactor, $S_\ell \sim (1/6)\ln[\Lambda R/(2\ell+1)]$ is seen for a massless 3+1D scalar field theory [see Fig. 1(d)], while the massive theories in 3+1D also show $S_\ell \sim R^0$ [see Fig. 1(f)]. In this case, a scaling with $\Lambda R/(2\ell+1)$ leads to a better data collapse. Thus, we see that in contrast to the total entanglement entropy, the leading scaling of S_ℓ with subsystem size can be used to distinguish between the gapped and the critical ground state of the scalar field theory. This is a key result of this paper.

The leading-order scaling of S_ℓ with subsystem size should also hold in an interacting theory, like a $O(N)$ theory [43], and can be used to detect a quantum phase transition in 2+1D or 3+1D theories [43,49]. As one approaches the quantum phase transition in this theory from the disordered side, one would expect $S_\ell \sim \ln[\Lambda R/2\ell]$ at the critical point. Close to the critical point, S_ℓ will show logarithmic growth till a scale $R/\ell \sim \xi$ before saturating. This correlation length ξ would be diverging as one approaches the transition.

IV. UNDERSTANDING THE AREA LAW IN S: COMPARISON WITH FREE FERMIONS

The logarithmic scaling of angular momentum resolved entanglement entropy of massless scalar fields naturally raises the question: Why is this signature of criticality washed out and we get an area law when we sum over the angular momentum channels to get the total entropy. This is especially intriguing since the total entanglement entropy of free fermions (another CFT) in $d > 1$ shows an "area-log" scaling. To understand this, it is instructive to compare and contrast the scalar field theory with a system of conformally invariant noninteracting spinless fermions in $d > 1$. The Hamiltonian of the free Fermi gas is

$$H = \sum_{\mathbf{k}} \frac{k^2 - k_F^2}{2m} c_{\mathbf{k}}^\dagger c_{\mathbf{k}}, \tag{7}$$

where $c_{\mathbf{k}}^\dagger$ creates a fermion with momentum $\mathbf{k}$. The ground state is a spherical Fermi sea of radius k_F, where k_F is related to the density ρ by $\rho = (\Omega_d/d(2\pi)^d)\, k_F^d$. The momentum distribution of the fermions $n_{\mathbf{k}} = \Theta(k_F - k)$ jumps from 1 to 0 at $k = k_F$. In this case, it is well known [2,28,61] that the entanglement entropy of the system is given by

$$S = -\mathrm{Tr}_A\left[\hat{C}\ln\hat{C} + (1-\hat{C})\ln(1-\hat{C})\right], \tag{8}$$

where

$$C(\mathbf{r},\mathbf{r}') = \langle c_{\mathbf{r}}^\dagger c_{\mathbf{r}'}\rangle = \int \frac{d^d\mathbf{k}}{(2\pi)^d}\, n_{\mathbf{k}}\, e^{i\mathbf{k}\cdot(\mathbf{r}-\mathbf{r}')} \tag{9}$$

is the one particle correlation function. When A is a "sphere" of radius R at the origin, one can consider the decomposition into angular momentum channels, $S = \sum_\ell g_\ell S_\ell$, where

$$S_\ell = -\mathrm{Tr}_r\left[\hat{C}_\ell \ln \hat{C}_\ell + (1-\hat{C}_\ell)\ln(1-\hat{C}_\ell)\right], \tag{10}$$

with

$$C_\ell(r,r') = (rr')^{-\nu}\int_0^{k_F} dk\, k\, J_{\ell+\nu}(kr)\, J_{\ell+\nu}(kr'). \tag{11}$$

In Figs. 1(g) and 1(h), we plot the variation of S_ℓ with $k_F R$ for different values of ℓ for free Fermi gas in $d = 2$ and $d = 3$, respectively. In both cases, we find that for $k_F R \gg \ell$, S_ℓ scales logarithmically with $k_F R$. In fact, we numerically find that,

$$S_\ell \sim \tfrac{1}{6} \ln[k_F R] \tag{12}$$

i.e., the universal prefactor of the 1+1D CFT makes a reappearance. Note that, unlike the scalar field theory, there is no

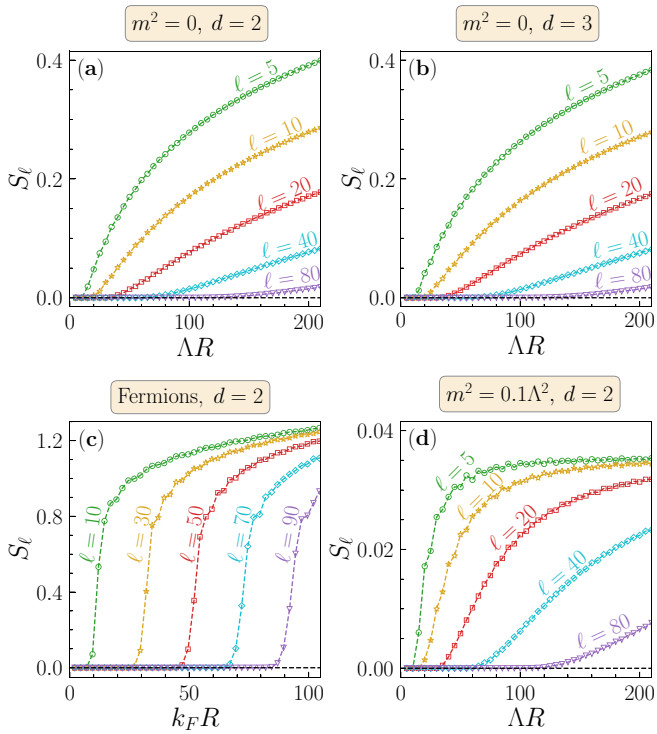

FIG. 2. Behavior of S_ℓ with subsystem size for large ℓ or small R: Massless scalar fields in 2+1D (a) and 3+1D (b): S_ℓ is strongly suppressed for $\Lambda R < 2\ell$ in 2+1D and $\Lambda R < 2\ell + 1$ in 3+1D. For a fixed ΛR, only $\ell < \ell_c$ contributes to S, where $2\ell_c \sim \Lambda R$. (c) S_ℓ for a free Fermi gas in $d = 2$ is strongly suppressed for $k_F R < \ell$. For a fixed $k_F R$, only $\ell < \ell_c$ contributes to S, where $\ell_c \sim k_F R$. The logarithmic scaling of S_ℓ together with the cutoff ℓ_c explains the leading scaling of S. (d) S_ℓ for a 2+1D massive scalar field theory with $m^2 = 0.1\Lambda^2$. The threshold of ΛR increases with ℓ, but $\ell_c/\Lambda R$ is not a universal number and varies weakly with ℓ.

additional scaling by ℓ in this case. The entanglement of a free Fermi gas is understood in terms of radial chiral modes at each angle on a Fermi surface [34]. Here we see that a similar argument holds for each angular momentum channel as well.

We now turn our attention to the reverse question: If S_ℓ shows logarithmic scaling with subsystem size for both the massless scalar fields and free Fermi gas, why does the entanglement entropy show an area law for the bosons and an area-log law for the fermions? To answer this question, we note that for the massless scalar fields in $d = 2$, S_ℓ is strongly suppressed for $2\ell \gg \Lambda R$ [see Fig. 2(a)]. So, for a given ΛR, only angular momentum channels with $\ell < \ell_c = \Lambda R/2$ contribute. For 3+1D critical scalar fields, a similar thresholding behavior is seen with $2\ell_c + 1 = \Lambda R$ [Fig. 2(b)]. The angular momentum ℓ corresponds to ℓ oscillations in the angular coordinate between 0 and 2π, with an angular period $\Delta\theta \sim 1/\ell$. This corresponds to the largest transverse wavelength in the subsystem $\Delta R_t \sim R\Delta\theta \sim R/\ell$. For $\ell \gg \Lambda R$, ΔR_t is much smaller than the short distance scale Λ^{-1}, and these fast transverse oscillations wash out the contribution of these modes to S. A similar thresholding behavior is also seen for the free Fermi gas with $\ell_c = k_F R$ [see Fig. 2(c) for $d = 2$ Fermi gas].

The area-log behavior of S for a free Fermi gas is now easy to understand: the number of ℓ modes scale as the area, $\sum_{\ell=0}^{k_F R} g_\ell \sim (k_F R)^{d-1}$ and each mode contributes $\sim \ln[k_F R]$. For the massless scalar field in 2+1D, a similar counting argument gives

$$S \sim \sum_{\ell}^{\Lambda R/2} \ln\left[\frac{\Lambda R}{2\ell}\right] \sim \frac{\Lambda R}{2}\ln\left[\frac{\Lambda R}{2}\right] - \ln\left[\frac{\Lambda R}{2}\right]! \sim \frac{\Lambda R}{2} + \text{const.} \tag{13}$$

The first term gives an area-log scaling similar to the fermions, but the second term gives $\ln(\Lambda R/2)! \sim (\Lambda R/2)\ln(\Lambda R/2) - (\Lambda R/2)$. The "area-log" terms cancel, leaving a leading-order area law scaling of S (see Appendix B). We note that this counting also correctly predicts that the next subleading term is a constant. A similar cancellation also occurs for $d = 3$ as well. In this case, we get

$$S \sim \sum_{\ell}^{(\Lambda R-1)/2} (2\ell+1)\ln\left[\frac{\Lambda R}{2\ell+1}\right] \sim \frac{(\Lambda R)^2}{48} + \frac{1}{72}\ln \Lambda R + \text{const.} \tag{14}$$

Here, there is an exact cancellation of both $\sim(\Lambda R)^2 \ln \Lambda R$ and $\sim \Lambda R \ln \Lambda R$ terms (see Appendix B for details). The counting not only correctly reproduces a leading nonuniversal area law scaling, but it also shows that in 3+1D, the first subleading term scales logarithmically with the system size (as is well known in the literature [35,42]). Thus, the extra factor of ℓ in the logarithmic scaling of S_ℓ leads to an exact cancellation of the universal terms, leaving a nonuniversal area law for entanglement entropy of critical bosons in $d > 1$. The scaling form also reproduces the fact that there are subleading logarithmic correction to S in 3+1D, while such correction is absent in 2+1D.

In Fig. 2(d), we plot the dependence of S_ℓ on ΛR for a massive scalar field theory with $m^2 = 0.1\Lambda^2$ in 2+1D. We again see thresholding, with the threshold in ΛR increasing with ℓ. However, $\ell_c/\Lambda R$ is not a universal number since the mass provides another length scale in the theory. Similar behavior is also seen in 3+1D massive theories. In this case, the area law can be explained by the number of angular momentum channels scaling with the area of the subsystem, with a constant contribution from each channel. Thus, although massive and massless scalar fields both show area law scaling of total entanglement entropy, they derive their origin from very different scaling of angular momentum resolved entanglement entropy. Angular momentum resolved entanglement is thus a more useful quantity to distinguish between gapped and critical phases.

V. FINITE TEMPERATURE BEHAVIOR OF S_ℓ: CROSSOVER FROM LOGARITHMIC TO LINEAR SCALING

Recent experiment in ultracold atoms [51], simultaneously measure the $\langle\phi(\mathbf{r},t)\phi(\mathbf{r}',t)\rangle$ and the $\langle\pi(\mathbf{r},t)\pi(\mathbf{r}',t)\rangle$ correlators to construct the entanglement entropy of $1d$ bosons. One can use similar measurements and Eq. (5) to construct $M_\ell^{\pm}(r,r')$ and hence S_ℓ for bosonic systems in $d > 1$. In

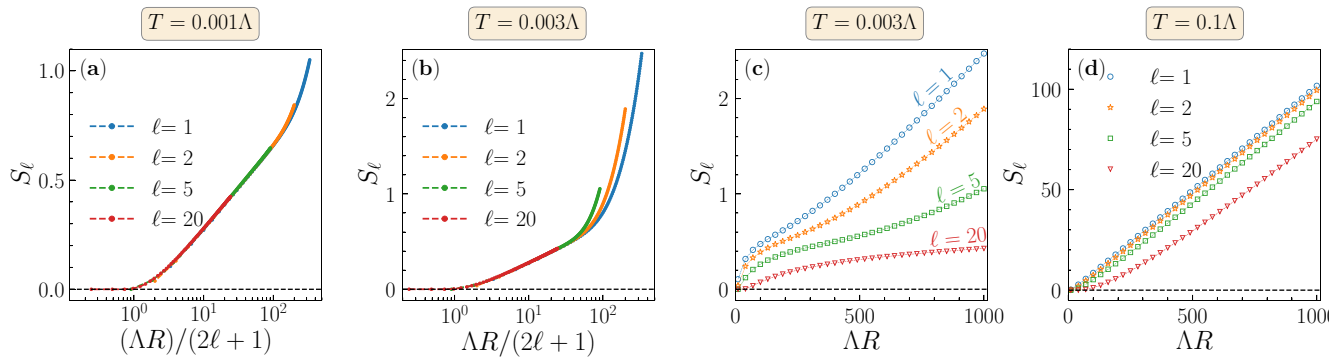

FIG. 3. Behavior of S_ℓ for massless scalar fields in 3+1D at three different finite temperatures (a) $T = 0.001\Lambda$, [(b) and (c)] 0.003Λ, and (d) 0.1Λ: (a) S_ℓ vs $\Lambda R/(2\ell+1)$ at low $T = 0.001\Lambda$: S_ℓ is strongly suppressed for $\Lambda R \leqslant 2\ell$. Then it increases with same logarithmic scaling behavior $S_\ell \sim (1/6)\ln[\Lambda R/(2\ell+1)]$ for a wide range of $R/(2\ell+1)$. For an intermediate temperature $T = 0.003\Lambda$, in (b), beyond the thresholding, there is a crossover in the scaling of S_ℓ from $S_\ell \sim (1/6)\ln[\Lambda R/(2\ell+1)]$ to $S_\ell \sim \pi TR/3$ in large ΛR, i.e., S_ℓ scales linearly with R in large R. The linear scaling becomes apparent when we look at the data in unscaled coordinate, i.e., S_ℓ vs ΛR in (c) for the same temperature. The log to linear crossover in the scaling of S_ℓ with subsystem size R happens at larger R for larger ℓ. At this temperature, $\ell = 1, 2$ and 5 have some part in the linear regime whereas $\ell = 20$ is still in the log scaling regime. Finally, at very high temperature, $T = 0.1\Lambda$ in (d), S_ℓ scales linearly with subsystem radius for all $\ell = 1, 2, 5, 20$, i.e., $S_\ell \sim \pi TR/3$.

this context, it is important to consider the finite-temperature behavior of S_ℓ (since the experiments operate at nonzero temperature). We would like to understand the stability of the logarithmic scaling behavior of S_ℓ at low T. More specifically, we wish to estimate the temperature ranges and subsystem sizes where one would see a remnant of the $T = 0$ logarithmic scaling. An important question in this regard is how these estimates depend on the angular momentum ℓ.

We first note that in a continuum model, where the thermodynamic limit of infinite system size has already been taken, the $\ell = 0$ mode of a 2+1D massless scalar field at finite T shows an infrared divergence and $S_{\ell=0}$ is not well defined. This is the same infrared divergence that leads to the Mermin-Wagner theorem prohibiting breaking of continuous global symmetries at finite T in 2+1D [62]. The $\ell \neq 0$ modes do not suffer from these infrared issues. In 3+1D, there are no infrared divergences for any ℓ channels at finite T.

In Fig. 3(a), we plot S_ℓ ($\ell = 1, 2, 5, 20$) as a function of $\Lambda R/(2\ell+1)$ (on a logarithmic scale) for a 3+1D critical scalar field theory at a finite temperature $T = 0.001\Lambda$. The curves for different ℓ collapses into a straight line in the intermediate logarithmic scaling regime, while deviating from each other at large ΛR. We find that S_ℓ shows the $T = 0$ logarithmic scaling with subsystem size R for all these ℓ values. For $\ell = 1$ and $\ell = 2$, we can see a bending towards a linear behavior at large $\Lambda R > 600$. In Figs. 3(b) and 3(c), we plot the behavior of S_ℓ with subsystem size for an intermediate $T = 0.003\Lambda$. In Fig. 3(b), we plot S_ℓ as a function of $\Lambda R/(2\ell+1)$ on a logarithmic scale, while in Fig. 3(c), the same data are plotted as a function of ΛR on a linear scale. It is clear that $S_\ell \sim \frac{1}{6}\ln[\Lambda R/(2\ell+1)]$ up to a lengthscale $R_c(\ell)$, beyond which it scales linearly with the subsystem radius (we numerically find that $S_\ell \sim \frac{\pi T}{3}R$), as expected for a 1+1D CFT at high temperatures. There is also a range of small subsystem sizes where S_ℓ shows thresholding behavior, but this region is hard to see in this figure. We find that with increasing values of ℓ, the range of subsystem sizes over which we see logarithmic behavior increases [see Fig. 3(c)], i.e., the logarithmic scaling remains more persistent for larger ℓ, e.g., for $\ell = 1$, the crossover occurs at $\Lambda R \sim 200$, while $\ell = 20$ shows logarithmic behavior all the way up to $\Lambda R = 1000$. If we lower the temperature, the region of logarithmic behavior increases, while raising the temperature leads to linear behavior for most values of ΛR. This is seen in Fig. 3(d), where we plot the behavior of S_ℓ with ΛR at a high temperature $T = 0.1\Lambda$. Here we find that S_ℓ (up to $\ell = 20$) shows linear behavior for almost all values of R. In general, one would expect an effective $T = 0$ logarithmic behavior for $R \ll \lambda_{\text{th}} \sim 1/T$ and a classical linear behavior for $R \gg \lambda_{\text{th}}$, where the thermal wavelength λ_{th} is the lengthscale over which the classical thermal fluctuations dephase the quantum interference effects. Figure 3(c) shows that the effective thermal dephasing length depends strongly on ℓ.

We now try to provide a more quantitative estimate of the temperature-dependent quantum-classical crossover, with a focus on the lengthscale where one can see the logarithmic behavior. For 3+1D, we fit the data for $S_\ell(R)$ in the regime $2 < \frac{\Lambda R}{2\ell+1} < \frac{\Lambda R^*}{2\ell+1}$ with a fitting function $S_\ell = \beta_\ell \log[\Lambda R/(2\ell+1)] + \text{const}$. For a given temperature T, we track the error of fit (through a coefficient of determination) as a function of R^* and define $R_c(T, \ell)$ as the largest value of R^* for which the error of fit is $\leqslant 2\%$. Thus, $2 < \frac{\Lambda R}{2\ell+1} < \frac{\Lambda R_c(T,\ell)}{2\ell+1}$ is the region where a logarithmic scaling can be seen at a temperature T within a 2% fitting error (see Appendix C for details). In Fig. 4, we plot $R_c(T)$ for different values of ℓ in $d = 3$. We see that R_c increases with decreasing temperature. We find that at very high temperature, R_c either saturates or increases. This region has to be discarded as the region over which fitting can reliably be done is very small and the analysis is error prone. Thus we find that beyond a maximum temperature $T_{\text{max}} \sim 0.02\Lambda$, the logarithmic region is not seen reliably. At this temperature $\Lambda R_c \sim 80$–120 for $\ell \sim 6$–10.

We finally consider the question of whether one can find a suitable parameter region in experiments with ultracold bosons to see the logarithmic scaling of S_ℓ. Let us first focus on $d = 3$, where there are no infrared divergences and a

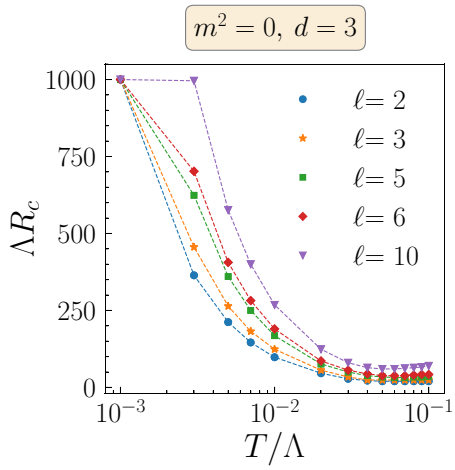

FIG. 4. Crossover scale $R_c(T)$ for the quantum-classical crossover of scaling of S_ℓ for different angular momentum channels as a function of the system temperature T in 3+1D. See text for details of determining $R_c(T)$. For $4\ell + 2 < \Lambda R < \Lambda R_c$ a logarithmic scaling can be seen with less than 2% error of fit.

BEC can be formed at finite T. The low-temperature BEC phase of the weakly interacting bosons is well described by Bogoliubov quasiparticles (Goldstone modes) with dispersion $E_{\mathbf{k}} = \sqrt{\hbar^2 c_s^2 k^2 + (\hbar^2 k^2/2m_B)^2}$, where c_s is the speed of sound in the medium and m_B is the mass of the boson (not to be confused with mass of scalar field). The momentum cutoff scale for the effective low-energy gapless scalar fields is then given by $\hbar c_s k_0 = \hbar^2 k_0^2/2m_B$, i.e., $k_0 = 2m_B c_s/\hbar$. Converting this to an energy scale, we then get $\Lambda = 2m_B c_s^2$. For a Na BEC, where $m_B = 3.817 \times 10^{-26}$ kg, and a typical speed of sound $c_s \sim 8$–12 mm/s is achievable [52], $k_0 \sim 8\,\mu\text{m}^{-1}$ and $\Lambda \sim 800$ nK (taking $c_s \sim 12$ mm/s). $T/\Lambda = 0.02$ in this case would correspond to $T = 16$ nK. Further, $k_0 R \sim 100$ corresponds to a radius of $\sim$12 μm. The typical operating temperature of ultracold bosons is $\sim$20 nK, and the trap lengthscales are $\sim$100–500 μm [51,52]. Thus, the limiting numbers we obtain are within the reach of current experiments and the critical logarithmic scaling can be verified up to $\ell = 10$. We however note that in $3d$, interference of atom clouds used to construct tomographic images is harder to achieve. Further the ultracold atom measurements typically integrate along a line of sight and this would be an issue in determining the correlations at each r and r'.

In contrast, the low T physics of ultracold bosons in $d = 2$ is more complicated. At the longest lengthscales, the harmonic trap changes the density of states and the system can beat the Mermin Wagner theorem to have a finite condensate fraction [63]. However, this is beyond our translation invariant scalar field description, and it remains an open issue whether S_ℓ in this case would still show logarithmic scaling. For systems where the presence of the trap can be ignored, the infrared divergence leads to Berezinskii-Kosterlitz-Thouless (BKT) physics [64–67], where the low T phase has a quasi-long-range order and vortices play a prominent role in determining the phase and phase transition [67,68]. This is also beyond a simple scalar field description. However, one can still measure a speed of sound, $c_s \sim 1$–2 mm/s [69] in Rb systems and even *if* we impose the same Bogoliubov description, we get $\Lambda \sim 90$ nK. $T/\Lambda \sim 0.02$ would then correspond to $T \sim 2$ nK, which is beyond the capability of current experiments.

VI. CONCLUSION

In this paper, we show that the scaling of angular momentum resolved entanglement entropy for a scalar field theory in $d > 1$ at $T = 0$ can distinguish between critical and gapped theories. For a critical theory in 2+1D, $S_\ell = \frac{1}{6}\ln[\Lambda R/2\ell]$ for $\ell \neq 0$ and $S_0 = \frac{1}{6}\ln[\Lambda R/2]$. In 3+1D, $S_\ell = \frac{1}{6}\ln[\Lambda R/(2\ell + 1)]$. The logarithmic scaling with the universal prefactor is a hallmark of a 1+1D CFT; however, the scaling here is with a scaled variable $\sim R/\ell$. The scaling holds for $\Lambda R \gg 2\ell$. For $\Lambda R \ll 2\ell$, S_ℓ drops precipitously and shows a thresholding behavior. In contrast, the massive theories show a logarithmic scaling till the finite correlation length is reached. Beyond the correlation length, $S_\ell \sim R^0$, i.e., it goes to a constant. Thus, unlike total entanglement entropy, which scales as an area law for both gapped and gapless phases, scaling of S_ℓ can be used to distinguish these theories.

We have also understood why the logarithmic scaling of S_ℓ leaves no signature in scaling of S in a critical bosonic theory, whereas a similar logarithmic scaling of S_ℓ leads to an area-log scaling of S in fermions. For both bosons and fermions, S_ℓ is negligible for $\Lambda R < 2\ell$ ($k_F R < \ell$). Thus, for a fixed R, the angular momentum sum is cutoff by $\ell_{\max} \sim R$, i.e., there are $\sim R^{d-1}$ such terms (note degeneracy factor of $2\ell + 1$ in 3+1D). For fermions, $S_\ell \sim \frac{1}{6}\ln[k_F R]$ for $k_F R > \ell$, and the angular momentum sum naturally leads to an area-log scaling. For bosons, the additional $\sim \ln \ell$ term gives rise to another area-log term which exactly cancels the first term, leaving a nonuniversal area law for S in 2+1D. In 3+1D, both a $(\Lambda R)^2 \ln \Lambda R$ and a $\Lambda R \ln \Lambda R$ term are exactly canceled, leaving a nonuniversal area law with a subleading logarithmic scaling with subsystem radius.

Finally, we show that at finite T, $S_\ell \sim \frac{\pi T}{3} R$ at large R and shows the $T = 0$ logarithmic scaling at low R (beyond thresholding). This quantum-classical crossover takes place at larger values of R for larger ℓ. We estimate that for $3d$ ultracold Bose gases, there is a range of available experimental parameters (in terms of size, temperature, etc.) where the logarithmic scaling of S_ℓ can be seen. This provides an opportunity to see and verify the scaling in ultracold atomic gases. In $2d$, infrared divergences and BKT physics complicate the analysis at finite temperatures. Harmonic traps provide a way to bypass Mermin-Wagner theorem, but the scale provided by the trap is likely to break the logarithmic scaling seen for the massless theories.

ACKNOWLEDGMENTS

M.K.S., S.M., and R.S. acknowledge the support of the Department of Atomic Energy, Government of India, for support under Project Identification No. RTI 4002. The authors acknowledge the use of computational facilities at the Department of Theoretical Physics, Tata Institute of Fundamental Research, Mumbai, for this paper.

M.K.S. and S.M. contributed equally to this work.

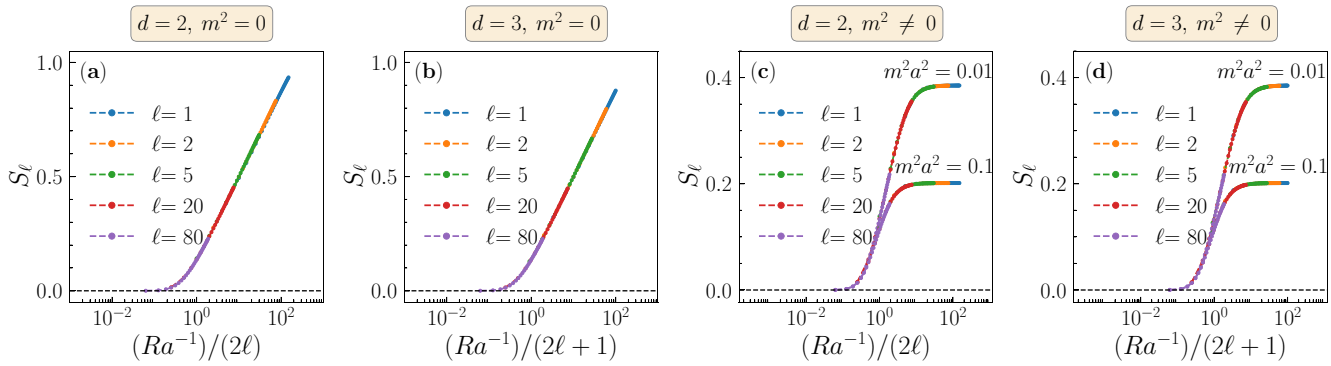

FIG. 5. Angular momentum resolved entanglement entropy S_ℓ of 2+1D and 3+1D scalar field theory using "Srednicki's regularization" on a finite lattice with lattice constant "a" for a spherical subsystem of size R. (a) Scaling of S_ℓ with $[Ra^{-1}/2\ell]$ for massless scalar field in $d = 2$. (b) Scaling of S_ℓ with $[Ra^{-1}/(2\ell + 1)]$ for massless scalar field in $d = 3$. (c) Scaling of S_ℓ with $[Ra^{-1}/2\ell]$ of massive scalar fields in $d = 2$ for $m^2a^2 = 0.01$ and 0.1. (d) Scaling of S_ℓ with $[Ra^{-1}/2\ell + 1]$ of massive scalar fields in $d = 3$ for $m^2a^2 = 0.01$ and 0.1.

APPENDIX A: ALTERNATE REGULARIZATION AND ROBUSTNESS OF RESULTS

It is well known [16,17,41] that the entanglement entropy of the ground state of a scalar field theory (both massive and massless) in $d > 1$ scales with the area of the subsystem, with a coefficient which is nonuniversal and depends on the regularization scheme. In the main text, we have shown that the angular momentum resolved entanglement, S_ℓ scales logarithmically with $\Lambda R/\ell$ for massless scalar fields. The natural question that arises is which of our results are dependent on the regularization scheme and which results are independent of it.

In the main text, we have used a regularization scheme with an ultraviolet momentum cutoff Λ and defined the fields in the continuum. The calculation of the angular momentum resolved entanglement entropy S_ℓ involves the calculation of eigenvalues of the correlation function $\hat{M}^2_\ell(r, r')$. While $\hat{M}^2$ is calculated as a continuum integral, we numerically evaluate it on a finite grid of equispaced radial points to construct a finite-dimensional matrix and consider its eigenvalues. While it is known that the continuum operator $\hat{M}^2_\ell$ has eigenvalues $\geqslant 1$ [2,17,56], the finite-dimensional matrix has spurious eigenvalues <1. We neglect these spurious eigenvalues and use only the eigenvalues $\geqslant 1$ for calculating the entanglement entropy. Our calculations do not change once the grid reaches Λ^{-1}. Note that the full system size is always set to infinity in our formulation.

One can use an alternate regularization scheme, as used by Srednicki in Refs. [16,41,42], where the radial Hamiltonian for each angular momentum channel $(\ell, \{m_\ell\})$ in d dimension becomes,

$$H_{\ell\{m_\ell\}} = \frac{1}{2}\int_0^\infty dr \left\{ \Pi^2_{\ell,\{m_\ell\}}(r) + r^{d-1}\left[\partial_r\left(\frac{\phi_{\ell,\{m_\ell\}}(r)}{r^{\frac{d-1}{2}}}\right)\right]^2 + \left[\frac{\ell(\ell+d-2)}{r^2} + m^2\right]\phi^2_{\ell,\{m_\ell\}}(r)\right\}. \tag{A1}$$

Here the fields $\phi_{\ell,\{m_\ell\}}$ and $\Pi_{\ell,\{m_\ell\}}$ are the projections of the scalar fields and their conjugate momenta into d dimensional spherical harmonics basis, satisfying $[\phi_{\ell,\{m_\ell\}}(r), \Pi_{\ell',\{m_{\ell'}\}}(r')] = i\delta_{\ell\ell'}\delta m_\ell m_{\ell'}\delta(r - r')$. The radial Hamiltonian is discretized on a finite lattice of N points with lattice constant a, which gives both UV and IR regularizations. The discrete Hamiltonian matrix is given by

$$H_{\ell\{m_\ell\}} = \frac{1}{2a}\sum_{i=1}^{N}\left\{\Pi^2_{\ell,\{m_\ell\},i} + \left(i + \frac{1}{2}\right)^{d-1}\left[\frac{\phi_{\ell,\{m_\ell\},i}}{(i)^{\frac{d-1}{2}}} - \frac{\phi_{\ell,\{m_\ell\},i+1}}{(i+1)^{\frac{d-1}{2}}}\right]^2 + \left[\frac{\ell(\ell+d-2)}{i^2} + m^2a^2\right]\phi^2_{\ell,\{m_\ell\},i}\right\}. \tag{A2}$$

One can then map this to a Hamiltonian of harmonic oscillators and use it to calculate the entanglement entropy. If there are N lattice points in the system and n lattice points in the subsystem, then one should consider the entanglement entropy in the limit $n/N \ll 1$ to get universal features.

In this section, we redo our calculations in the regularization scheme of Srednicki to show:

(1) For massless fields, $S_\ell \sim \frac{1}{6}\ln[\Lambda R/2\ell]$ is independent of regularization scheme (including the prefactor of 1/6). Subleading terms depend on the regularization scheme.

(2) For massive fields, $S_\ell \sim R^0$ scaling is independent of the regularization scheme, but the constant value reached by S_ℓ for massive theories depends on the regularization scheme.

(3) Hence the coefficient of the area law for S depends on the regularization scheme.

In Figs. 5(a) and 5(b), we plot S_ℓ for 2+1D and 3+1D massless scalar fields, obtained in the alternate lattice regularization, as a function of $Ra^{-1}/(2\ell)$ and $Ra^{-1}/(2\ell + 1)$, respectively. We find that $S_\ell \sim \frac{1}{6}\ln[\frac{Ra^{-1}}{2\ell}]$ in 2+1D and $S_\ell \sim \frac{1}{6}\ln[\frac{Ra^{-1}}{2\ell+1}]$ in 3+1D, respectively. This matches with our results with $a \sim \Lambda^{-1}$. We have taken $N = 1000$ and n up to 300 for these plots. In Figs. 5(c) and 5(d), we plot S_ℓ for massive scalar fields in $d = 2$ and $d = 3$, respectively. We see that S_ℓ saturates to a constant, which decreases with increasing m. However, the value of the constant is different in the two regularization schemes: e.g., in $d = 2$, in our scheme, the constant value of $S_\ell \sim 0.17$ for $m^2 = 0.01\Lambda^2$, while the Srednicki regularization scheme gives $S_\ell \sim 0.39$ for $m^2 = 0.01a^{-2}$. This

results in the coefficient of the area law for total entanglement entropy being regularization dependent. Thus, our key results are robust to the vagaries of the regularization schemes used to calculate the entanglement entropy.

APPENDIX B: TOTAL ENTANGLEMENT ENTROPY (S) FROM S_ℓ: ANGULAR MOMENTUM SUM

In the main text, we stated that the logarithmic scaling of S_ℓ with $\Lambda R/\ell$, together with a cutoff $\ell_c \sim \Lambda R$, leads to a cancellation of two "area-log" terms in the scaling of total entanglement entropy, leaving an area law with nonuniversal coefficients even for the massless scalar field. In this Appendix, we provide the details of these calculations.

For the gapless scalar field in 2+1D, we have shown in the main text,

$$S_\ell \sim \frac{1}{6}\left\{\ln\left(\frac{\Lambda R}{2\ell}\right) - \ln B\right\}\Theta\left[\ln\left(\frac{\Lambda R}{2\ell}\right) - \ln B\right]. \quad \text{(B1)}$$

for $\ell \neq 0$. Here B is an $O(1)$ number and the Θ function gives an upper limit $\ell_c = (\frac{\Lambda R}{2B})$ of the angular momentum channels which adds a nonzero contribution to the entropy for a fixed system size ΛR. Note that, this approximate scaling function is not quantitatively accurate near the transition region where each of the ℓ channels starts rising to nonzero values from zero, but these inaccuracies give us subleading corrections. Additionally, we have found that $S_{\ell=0} \sim \frac{1}{6}\ln(\frac{\Lambda R}{2B})$. With this ansatz, the total entanglement entropy,

$$\begin{aligned}
S &\sim \frac{1}{6}\sum_{\ell=1}^{\ell_c} 2\left[\ln\left(\frac{\Lambda R}{2\ell}\right) - \ln B\right] + \frac{1}{6}\ln\left(\frac{\Lambda R}{2B}\right) \\
&= \frac{1}{3}\sum_{\ell=1}^{\ell_c}\ln\left(\frac{\ell_c}{\ell}\right) + \frac{1}{6}\ln\left(\frac{\Lambda R}{2B}\right) \\
&= \frac{1}{3}[\ell_c \ln(\ell_c) - \ln(\ell_c!)] + \frac{1}{6}\ln(\ell_c) \\
&\approx \frac{1}{3}\left[\ell_c - \frac{1}{2}\ln(\ell_c) - \frac{1}{2}\ln(2\pi) + \ldots\right] + \frac{1}{6}\ln(\ell_c) \\
&= \frac{1}{6B}(\Lambda R) + \text{const.} \qquad \text{(B2)}
\end{aligned}$$

In the second last line of (B2), we have used the Stirling approximation. Note that, the "area-log" term $\ell_c \ln \ell_c$ is exactly canceled by the leading-order term in the Stirling approximation of $\ln(\ell_c!)$ thereby leaving an area law in 2+1D. Also, the contribution of the $\ell = 0$ mode exactly cancels the subleading $\ln \ell_c$ term in the Stirling approximation. This explains the absence of subleading logarithmic term in total entanglement entropy S in 2+1D in contrast to 3+1D where we do get a logarithmic subleading term. Indeed, using this scaling function we get area law for 2+1D, i.e., the entanglement entropy increases linearly with the subsystem size showing an area law.

For the gapless scalar field in 3+1D, we have shown in the main text,

$$S_\ell \sim \frac{1}{6}\left\{\ln\left(\frac{\Lambda R}{2\ell+1}\right) - \ln B\right\}\Theta\left[\ln\left(\frac{\Lambda R}{2\ell+1}\right) - \ln B\right]. \quad \text{(B3)}$$

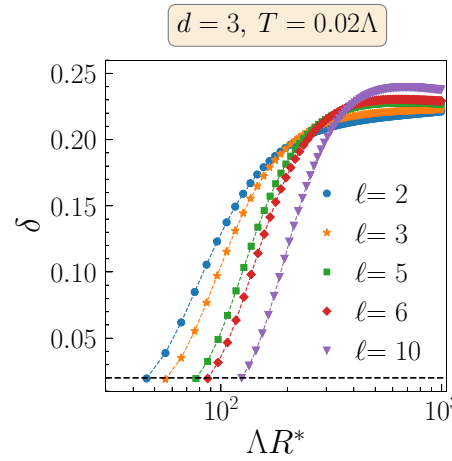

FIG. 6. Fitting Error $\delta = 1 - R_d^2$ as a function of R^* for temperature $T = 0.02\Lambda$ in 3+1D. Value of $R_c(T)$ is the value R^* for which the error of fit is $\leqslant 2\%$.

Here B is an $O(1)$ number and the Θ function gives an upper limit $\ell_c = (\frac{\Lambda R}{2B} - \frac{1}{2})$ of the angular momentum channels which adds a nonzero contribution to the entropy for a fixed system size ΛR. With this ansatz,

$$\begin{aligned}
S &\sim \frac{1}{6}\sum_{\ell=0}^{\ell_c}(2\ell+1)\left[\ln\left(\frac{\Lambda R}{2\ell+1}\right) - \ln B\right] \\
&= \frac{1}{6}\left[(\ell_c+1)^2\ln(2\ell_c+1) - \sum_{\ell=0}^{\ell_c}(2\ell+1)\ln(2\ell+1)\right] \\
&= \frac{1}{6}\left\{\left[(\ell_c)^2\ln(2\ell_c) + \frac{\ell_c}{2} + (2\ell_c)\ln(2\ell_c) + \ln(\ell_c) + \cdots\right]\right. \\
&\quad - \left[(\ell_c)^2\ln(2\ell_c) - \frac{{\ell_c}^2}{2} + (2\ell_c)\ln(2\ell_c)\right. \\
&\quad \left.\left. + \frac{11}{12}\ln(\ell_c) + \cdots\right]\right\} \\
&= \frac{1}{6}\left[\frac{\ell_c(\ell_c+1)}{2} + \frac{1}{12}\ln(\ell_c) + \cdots\right] \\
&\approx \frac{1}{48B^2}(\Lambda R)^2 + \frac{1}{72}\ln(\Lambda R) + \text{const.} \qquad \text{(B4)}
\end{aligned}$$

Note the cancellation of both $\ell_c^2 \ln \ell_c$ and $\ell_c \ln \ell_c$ terms in the second line of (B4). Hence, the "area-log" term is exactly canceled in this case too leaving the leading area law along with the subleading logarithmic correction in 3+1D. Thus, these simple scaling ansatz of S_ℓ not only explains the leading area law but also explains the absence of subleading logarithmic term in $d = 2$, in contrast to the presence of such term in $d = 3$.

APPENDIX C: R_c ESTIMATION THROUGH A COEFFICIENT OF DETERMINATION

In the main text, we have given an estimate of R_c obtained via tracking the error of fit through a coefficient of determination. For a given data set $S_\ell(R_i)$ of n number of

points for which we fit a function $f_\ell(R_i)$, the coefficient of determination(R_d) is defined as $R_d^2 = 1 - \frac{S_{\rm res}}{S_{\rm tot}}$. Here $S_{\rm res} = \sum_{i=1}^{n}[S_\ell(R_i) - f_\ell(R_i)]^2$ is the sum of squares of residuals and $S_{\rm tot} = \sum_{i=1}^{n}[S_\ell(R_i) - \bar{S}_\ell]^2$ is proportional to the variance with respect to average value $\bar{S}_\ell = \frac{1}{n}\sum_{i=1}^{n} S_\ell(R_i)$ of the data set.

We track $\delta = 1 - R_d^2$ as the error in the fitting of S_ℓ for different values of R^* and keep decreasing R^* until we reach an error of 2% for a fitting function $f_\ell(R) = \beta_\ell \ln[\Lambda R/(2\ell + 1)] + \text{const.}$ in the range $2 < \frac{\Lambda R}{2\ell+1} < \frac{\Lambda R^*}{2\ell+1}$. We define $R_c(T)$ as the largest value of R^* for which the error of fit is $\leqslant 2\%$. In Fig. 6, we plot δ as a function of R^* for 3+1D at a temperature $T = 0.02\Lambda$. Error δ decreases with decreasing R^*. At this temperature $T = 0.02\Lambda$, crossover scale $\Lambda R_c \sim 85$–120 for $\ell \sim 6$–10.

[1] N. Laflorencie, Quantum entanglement in condensed matter systems, Phys. Rep. **646**, 1 (2016).

[2] H. Casini and M. Huerta, Entanglement entropy in free quantum field theory, J. Phys. A: Math. Theor. **42**, 504007 (2009).

[3] L. Amico, R. Fazio, A. Osterloh, and V. Vedral, Entanglement in many-body systems, Rev. Mod. Phys. **80**, 517 (2008).

[4] J. Eisert, M. Cramer, and M. B. Plenio, Colloquium: Area laws for the entanglement entropy, Rev. Mod. Phys. **82**, 277 (2010).

[5] H.-C. Jiang, Z. Wang, and L. Balents, Identifying topological order by entanglement entropy, Nat. Phys. **8**, 902 (2012).

[6] A. Kitaev and J. Preskill, Topological entanglement entropy, Phys. Rev. Lett. **96**, 110404 (2006).

[7] T. Grover, A. M. Turner, and A. Vishwanath, Entanglement entropy of gapped phases and topological order in three dimensions, Phys. Rev. B **84**, 195120 (2011).

[8] M. Levin and X.-G. Wen, Detecting topological order in a ground state wave function, Phys. Rev. Lett. **96**, 110405 (2006).

[9] P. Fromholz, G. Magnifico, V. Vitale, T. Mendes-Santos, and M. Dalmonte, Entanglement topological invariants for one-dimensional topological superconductors, Phys. Rev. B **101**, 085136 (2020).

[10] G. Vidal, J. I. Latorre, E. Rico, and A. Kitaev, Entanglement in quantum critical phenomena, Phys. Rev. Lett. **90**, 227902 (2003).

[11] M. P. Hertzberg and F. Wilczek, Some calculable contributions to entanglement entropy, Phys. Rev. Lett. **106**, 050404 (2011).

[12] P. Calabrese and J. Cardy, Entanglement entropy and quantum field theory, J. Stat. Mech.: Theory Exp. (2004) P06002.

[13] H. Ma, A. T. Schmitz, S. A. Parameswaran, M. Hermele, and R. M. Nandkishore, Topological entanglement entropy of fracton stabilizer codes, Phys. Rev. B **97**, 125101 (2018).

[14] Q. Miao and T. Barthel, Eigenstate entanglement: Crossover from the ground state to volume laws, Phys. Rev. Lett. **127**, 040603 (2021).

[15] A. Chakraborty and R. Sensarma, Renyi entropy of interacting thermal bosons in the large-n approximation, Phys. Rev. A **104**, 032408 (2021).

[16] A. Riera and J. I. Latorre, Area law and vacuum reordering in harmonic networks, Phys. Rev. A **74**, 052326 (2006).

[17] L. Bombelli, R. K. Koul, J. Lee, and R. D. Sorkin, Quantum source of entropy for black holes, Phys. Rev. D **34**, 373 (1986).

[18] M. B. Hastings, An area law for one-dimensional quantum systems, J. Stat. Mech.: Theory Exp. (2007) P08024.

[19] D. A. Abanin, E. Altman, I. Bloch, and M. Serbyn, Colloquium: Many-body localization, thermalization, and entanglement, Rev. Mod. Phys. **91**, 021001 (2019).

[20] B. Bauer and C. Nayak, Area laws in a many-body localized state and its implications for topological order, J. Stat. Mech.: Theory Exp. (2013) P09005.

[21] A. Pal and D. A. Huse, Many-body localization phase transition, Phys. Rev. B **82**, 174411 (2010).

[22] R. Nandkishore and D. A. Huse, Many body localization and thermalization in quantum statistical mechanics, Annu. Rev. Condens. Matter Phys. **6**, 15 (2015).

[23] D. J. Luitz, N. Laflorencie, and F. Alet, Many-body localization edge in the random-field Heisenberg chain, Phys. Rev. B **91**, 081103(R) (2015).

[24] C. J. Turner, A. A. Michailidis, D. A. Abanin, M. Serbyn, and Z. Papić, Quantum scarred eigenstates in a Rydberg atom chain: Entanglement, breakdown of thermalization, and stability to perturbations, Phys. Rev. B **98**, 155134 (2018).

[25] W. W. Ho, S. Choi, H. Pichler, and M. D. Lukin, Periodic orbits, entanglement, and quantum many-body scars in constrained models: Matrix product state approach, Phys. Rev. Lett. **122**, 040603 (2019).

[26] W. W. Ho and D. A. Abanin, Entanglement dynamics in quantum many-body systems, Phys. Rev. B **95**, 094302 (2017).

[27] A. Chakraborty and R. Sensarma, Nonequilibrium dynamics of Renyi entropy for bosonic many-particle systems, Phys. Rev. Lett. **127**, 200603 (2021).

[28] S. Moitra and R. Sensarma, Entanglement entropy of fermions from Wigner functions: Excited states and open quantum systems, Phys. Rev. B **102**, 184306 (2020).

[29] P. Calabrese and J. Cardy, Entanglement entropy and conformal field theory, J. Phys. A: Math. Theor. **42**, 504005 (2009).

[30] M. Saravani, R. D. Sorkin, and Y. K. Yazdi, Spacetime entanglement entropy in 1 + 1 dimensions, Class. Quantum Grav. **31**, 214006 (2014).

[31] C. Callan and F. Wilczek, On geometric entropy, Phys. Lett. B **333**, 55 (1994).

[32] C. Holzhey, F. Larsen, and F. Wilczek, Geometric and renormalized entropy in conformal field theory, Nucl. Phys. B **424**, 443 (1994).

[33] D. Gioev and I. Klich, Entanglement entropy of fermions in any dimension and the widom conjecture, Phys. Rev. Lett. **96**, 100503 (2006).

[34] B. Swingle, Conformal field theory approach to fermi liquids and other highly entangled states, Phys. Rev. B **86**, 035116 (2012).

[35] S. Ryu and T. Takayanagi, Aspects of holographic entanglement entropy, J. High Energy Phys. 08 (2006) 045.

[36] E. Fradkin and J. E. Moore, Entanglement entropy of 2D conformal quantum critical points: Hearing the shape of a quantum drum, Phys. Rev. Lett. **97**, 050404 (2006).

[37] T. Barthel, M.-C. Chung, and U. Schollwöck, Entanglement scaling in critical two-dimensional fermionic and bosonic systems, Phys. Rev. A **74**, 022329 (2006).

[38] W. Li, L. Ding, R. Yu, T. Roscilde, and S. Haas, Scaling behavior of entanglement in two- and three-dimensional free-fermion systems, Phys. Rev. B **74**, 073103 (2006).
[39] M. M. Wolf, Violation of the entropic area law for fermions, Phys. Rev. Lett. **96**, 010404 (2006).
[40] P. Calabrese, M. Mintchev, and E. Vicari, Entanglement entropies in free-fermion gases for arbitrary dimension, Europhys. Lett. **97**, 20009 (2012).
[41] M. Srednicki, Entropy and area, Phys. Rev. Lett. **71**, 666 (1993).
[42] R. Lohmayer, H. Neuberger, A. Schwimmer, and S. Theisen, Numerical determination of entanglement entropy for a sphere, Phys. Lett. B **685**, 222 (2010).
[43] M. A. Metlitski, C. A. Fuertes, and S. Sachdev, Entanglement entropy in the $O(N)$ model, Phys. Rev. B **80**, 115122 (2009).
[44] H. Casini and M. Huerta, Entanglement and alpha entropies for a massive scalar field in two dimensions, J. Stat. Mech.: Theory Exp. (2005) P12012.
[45] M. Goldstein and E. Sela, Symmetry-resolved entanglement in many-body systems, Phys. Rev. Lett. **120**, 200602 (2018).
[46] S. Fraenkel and M. Goldstein, Symmetry resolved entanglement: Exact results in 1D and beyond, J. Stat. Mech.: Theory Exp. (2020) 033106.
[47] D. Katsinis and G. Pastras, An inverse mass expansion for entanglement entropy in free massive scalar field theory, Eur. Phys. J. C **78**, 282 (2018).
[48] M. Huerta and G. van der Velde, Modular Hamiltonian of the scalar in the semi infinite line: Dimensional reduction for spherically symmetric regions, J. High Energy Phys. 06 (2023) 097.
[49] S. Whitsitt, W. Witczak-Krempa, and S. Sachdev, Entanglement entropy of large-N Wilson-Fisher conformal field theory, Phys. Rev. B **95**, 045148 (2017).
[50] R. Islam, R. Ma, P. M. Preiss, M. Eric Tai, A. Lukin, M. Rispoli, and M. Greiner, Measuring entanglement entropy in a quantum many-body system, Nature (Lond.) **528**, 77 (2015).
[51] M. Tajik, I. Kukuljan, S. Sotiriadis, B. Rauer, T. Schweigler, F. Cataldini, J. Sabino, F. Møller, P. Schüttelkopf, S.-C. Ji, D. Sels, E. Demler, and J. Schmiedmayer, Verification of the area law of mutual information in a quantum field simulator, Nat. Phys. **19**, 1022 (2023).
[52] M. R. Andrews, D. M. Kurn, H.-J. Miesner, D. S. Durfee, C. G. Townsend, S. Inouye, and W. Ketterle, Propagation of sound in a Bose-Einstein condensate, Phys. Rev. Lett. **79**, 553 (1997).
[53] I. Bloch, J. Dalibard, and W. Zwerger, Many-body physics with ultracold gases, Rev. Mod. Phys. **80**, 885 (2008).
[54] W. Ketterle, Nobel lecture: When atoms behave as waves: Bose-Einstein condensation and the atom laser, Rev. Mod. Phys. **74**, 1131 (2002).
[55] A. Botero and B. Reznik, Spatial structures and localization of vacuum entanglement in the linear harmonic chain, Phys. Rev. A **70**, 052329 (2004).
[56] M. B. Plenio, J. Eisert, J. Dreißig, and M. Cramer, Entropy, entanglement, and area: Analytical results for harmonic lattice systems, Phys. Rev. Lett. **94**, 060503 (2005).
[57] P. Bueno, R. C. Myers, and W. Witczak-Krempa, Universality of corner entanglement in conformal field theories, Phys. Rev. Lett. **115**, 021602 (2015).
[58] E. M. Stoudenmire, P. Gustainis, R. Johal, S. Wessel, and R. G. Melko, Corner contribution to the entanglement entropy of strongly interacting O(2) quantum critical systems in 2+1 dimensions, Phys. Rev. B **90**, 235106 (2014).
[59] J. Helmes and S. Wessel, Entanglement entropy scaling in the bilayer Heisenberg spin system, Phys. Rev. B **89**, 245120 (2014).
[60] N. Laflorencie, D. J. Luitz, and F. Alet, Spin-wave approach for entanglement entropies of the $J_1 - J_2$ Heisenberg antiferromagnet on the square lattice, Phys. Rev. B **92**, 115126 (2015).
[61] I. Peschel and V. Eisler, Reduced density matrices and entanglement entropy in free lattice models, J. Phys. A: Math. Theor. **42**, 504003 (2009).
[62] A. Altland and B. Simons, *Condensed Matter Field Theory* (Cambridge University Press, Cambridge, UK, 2023).
[63] C. Pethick and H. Smith, *Bose-Einstein Condensation in Dilute Gases* (Cambridge University Press, Cambridge, UK, 2008).
[64] J. M. Kosterlitz and D. J. Thouless, Ordering, metastability and phase transitions in two-dimensional systems, J. Phys. C **6**, 1181 (1973).
[65] V. L. Berezinsky, Destruction of long-range order in one-dimensional and two-dimensional systems possessing a continuous symmetry group. II. Quantum systems., Sov. Phys. JETP **34**, 610 (1972).
[66] Z. Hadzibabic, P. Krüger, M. Cheneau, B. Battelier, and J. Dalibard, Berezinskii–Kosterlitz–Thouless crossover in a trapped atomic gas, Nature (Lond.) **441**, 1118 (2006).
[67] L. Mathey, K. J. Günter, J. Dalibard, and A. Polkovnikov, Dynamic Kosterlitz-Thouless transition in two-dimensional Bose mixtures of ultracold atoms, Phys. Rev. A **95**, 053630 (2017).
[68] Z. Hadzibabic and J. Dalibard, *Bkt Physics with Two-Dimensional Atomic Gases* (World Scientific, Singapore, 2012), pp. 297–323.
[69] J. L. Ville, R. Saint-Jalm, E. Le Cerf, M. Aidelsburger, S. Nascimbène, J. Dalibard, and J. Beugnon, Sound propagation in a uniform superfluid two-dimensional Bose gas, Phys. Rev. Lett. **121**, 145301 (2018).